

# Fabrication and Characterization of n-ZnS/p-Si and n-ZnS:Al/p-Si Heterojunction

Eman M. Nasir

**Abstract**— A thin films of ZnS and ZnS:Al with various Al concentration (0, 1, 2)%wt has been prepared successfully. Also n-ZnS/p-Si and n-ZnS:Al/p-Si heterojunction detector(HJ<sub>s</sub>) has been fabricated by thermal evaporation at different Al concentration. Structure of these films was characterized by X-ray diffraction. The structures of these films are cubic zinc along (111) plane The reverse bias capacitance was measured as a function of bias voltage, and it is indicated that these HJ<sub>s</sub> are abrupt. The capacitance decreases with increasing the reverse bias, and fixed at high value of reverse bias voltage. The capacitance increases with increasing Al concentration. The width of depletion layers decreases with increases Al concentration. The value of highest built in potential varies between (2-1.37V). The current-voltage characteristic of n-ZnS/p-Si and n-ZnS:Al/p-Si heterojunction show that the forward current at dark condition varies approximately exponentially with applied voltage and the junction was coincide with recombination-tunneling model, and reverse current exhibited a soft breakdown. The difference between forward and reverse current with applied voltage indicates that the detector has a high rectification characteristic. The value of ideality factor was varies between 2.58-3.22, and the value of tunneling constant ( $A_0$ ) varies between 4.92-8.05V<sup>-1</sup>. From the I-V measurements under illumination, the photocurrent increased with increasing Al concentration. The energy band diagram for HJ has been constructed

**Index Terms**— C-V measurements, heterojunction, vacuum evaporation, Zinc sulfide.

## I. INTRODUCTION

Zinc sulfide (ZnS) was one of the first semiconductors discovered and is also an important semiconductor material with direct wide band gaps for cubic and hexagonal phases of 3.72 and 3.77 eV, respectively. It has a high absorption coefficient in the visible range of the optical spectrum and reasonably good electrical properties. This property makes ZnS very attractive as an absorber in heterojunction thin-film solar cells. Furthermore, ZnS also offers the advantage of being a nontoxic semiconductor material (without Cd and Pb). These doped ZnS semiconductor materials have a wide range of applications in electroluminescence devices, phosphors, light emitting displays, and optical sensors. Doped nanoparticles of dimensions below Bohr diameter exhibit interesting optoelectronic properties due to quantum size effect and are potential candidates for variety of applications. The characteristics and concentrations of dopants are responsible for particular luminescence emission and efficiency of semiconductor nanoparticles.

Hence investigation of the role of dopant concentration on optical properties of doped semiconductor nanoparticles is very important from the viewpoints of basic physics as well as applications[1-5]. Recently, 2D nanostructure P-N junctions have attracted a great deal of attention for their potential applications in photovoltaic device.

In recent years, ZnS thin films have been grown by a variety of deposition techniques, such as chemical bath deposition, evaporation, and solvothermal method. Chemical bath deposition is promising because of its low cost, arbitrary substrate shapes, simplicity, and capability of large area preparation. There are many reports of successful fabrication of ZnS-based heterojunctionsolar cells by the chemical bath deposition method, such as with CIGS used for the n-type emitter layer [2-7]

ZnS/Si heterojunctions(HJ) have been extensively studied for the wide extent of their application in electronic and optoelectronic devices such as detector lasers and solar cells. Anderson fabricated the first isotype and anisotype HJ in 1960, this is achieved by means of the HJ window effect [3,4]. Anderson model is one of the earliest theoretical models for the behavior of the abrupt HJ based on the approximation, while the other models include the effect of interface state, dipoles and tunneling. Indeed the properties of the interface vary greatly due to variations in material parameters and fabrication method [3-11]. Moreover, ZnS also has the advantage of being perfectly lattice matched with Si substrates (0.2%), which makes it a promising material for the integration of optoelectronic devices onto Si substrates. The most promising advantage of the ZnS/Si heterostructure is the ability to combine the optoelectronic properties of ZnS with the high-density circuit capabilities of Si. Up to now, few investigations on the UV and visible photoresponse properties of n-ZnS/p-Si heterojunction

are available. In this study, an n-ZnS/ p- Si heterojunction diode was fabricated by depositing an n-type ZnS film on a p-type Si substrate by using the rf magnetron sputtering method. The optical and electrical properties of the heterojunction are reported and discussed.[12].

The aim of this work is to fabricate ZnS/Si and ZnS:Al/Si photovoltaic HJ by thermal evaporation technique, and studying the effect of Al concentration on it is electrical, and photovoltaic HJ properties.

## II. EXPERIMENTAL WORK

The ZnS and ZnS:Al thin films have been prepared by vacuum evaporation technique on Si substrate using Edward E306A under lower pressure of about 10<sup>-6</sup>mbar with (0.8)μm thickness, heat treatment has been used in vacuum by electric furnace at 400K. n-ZnS/p-Si and n-ZnS:Al/p-Si heterojunction detector are fabricated with

Manuscript received December, 2013.

Eman M. Nasir, Physics Department, University of Baghdad/ College of Science/ Baghdad university, Baghdad, Iraq.

different value of Al concentration as shown in Fig. 1. The structure of these films grown on Si substrates was examined by a phillips x-ray diffractometer with copper  $K_{\alpha}$  radiation of the wavelength ( $\lambda=1.541 \text{ \AA}$ ). I-V characteristics with dark for PV (at forward and reverse bias) and C-V characteristics have been measured with different Al concentration (pure, 1%, 2%).

The C-V measurement is useful to determine the type of the heterojunction (abrupt or graded), built-in potential ( $V_{bi}$ ), concentration and the width of junction by using LRC meters model HP-R2CC4274A and 4275A, from measuring the capacitance of n-ZnS/p-Si and n-ZnS:Al/p-Si heterojunction films as a function of reverse bias(0-5)V, the value of  $V_{bi}$  can be found from plots the relation between  $1/C^2$  and reverse bias, then the interception of the straight line with voltage axis is represents the built-in voltage. The concentration of carrier can be determined from the relation:

$$1/C^2 = [2(\epsilon_1 N_{A1} + \epsilon_2 N_{D2}) / q N_{D2} N_{A1} \epsilon_1 \epsilon_2] (V_{bi} - V_a) \quad (1)$$

Where  $[2(\epsilon_1 N_{A1} + \epsilon_2 N_{D2}) / q N_{D2} N_{A1} \epsilon_1 \epsilon_2]$  is represent the slope. The current-voltage measurements in the dark have been measured by using Keithly Digital Electrometer 616 and D.C power supply.

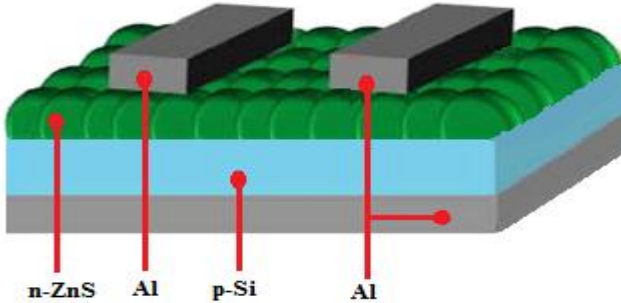


Figure 1: Schematic represent the n-ZnS/p-Si heterojunction

### III. RESULTS AND DISCUSSION

Fig. 2 shows the x-ray diffraction pattern of the n-ZnS/p-Si heterojunction at Al concentration of (pure, 1%, 2%). Only one XRD peak located at about 28.76- 28.58 corresponding to the cubic (111) reflection was observed from these samples (Joint Committee on Powder Diffraction Standard, JCPDS Card No. 77-2100),, which indicates that the film is strongly oriented.[8] The preferred orientation and peak with low full-width at half-maximum (FWHM) (about 0.2-0.5) are indicative of the good crystallinity of the ZnS film. Similar results are reported by other researchers [5-8]. The intensity of the diffraction peak is increased with doped with Al, which illuminates the enhancement of crystallinity and grain size of ZnS:Al thin films. With the increase of Al concentration, The capacitance-voltage characteristics have been studied. The variation of capacitance as a function of reverse bias voltage (0-5)V for n-ZnS/p-Si and n-ZnS:Al/p-Si at different Al concentration (pure, 1%, 2%)wt) are shown in Fig. 3. It is observed that the capacitance decreases with increasing the reverse bias, and this is in agreement with equation

$$C/A = [q N_{D2} N_{A1} \epsilon_1 \epsilon_2 / 2(\epsilon_1 N_{A1} + \epsilon_2 N_{D2})]^{1/2} (V_{bi} - V_a)^{-1/2} \quad (1)$$

This decreasing was non-linear as shown in Fig. 3. This behavior was attributed to the increasing in the depletion region width which leading to increasing the value of built-in voltage according to the equation:.

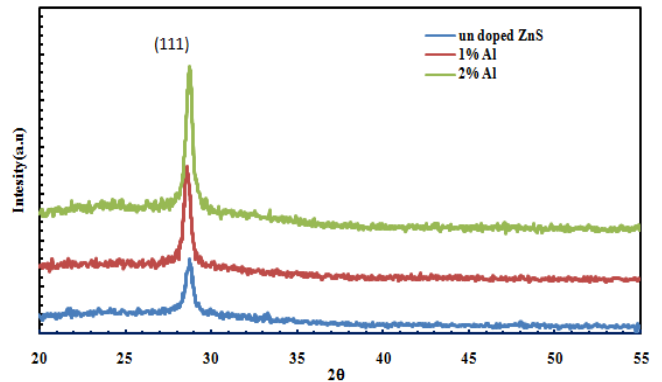


Figure 2: XRD patterns of pure ZnS/Si and ZnS:Al/Si thin films at Al concentration of 1%, 2%

$$C = dQ/dV_a = \epsilon_s/W \quad (2)$$

We can see from Fig. 3 that the capacitance increases with increasing Al concentration from pure to 2% and this attributed to increase the surface state which leading to the decrease in the depletion layer and increasing in the capacitance as in table I.

The width of the depletion layer (W) can be calculated by the equation:

$$W = \epsilon_s / C_o \quad (3)$$

where  $C_o$  is the capacitance at zero bias voltage and

$$(\epsilon_s = \epsilon_n \epsilon_p / \epsilon_n \epsilon_p) \quad (4)$$

where  $\epsilon_p$  is the dielectric constant for Si and  $\epsilon_n$  is the dielectric constant for ZnS. table I shows the variation of the width of the depletion layer for n-ZnS/p-Si and n-ZnS:Al/p-Si at different Al

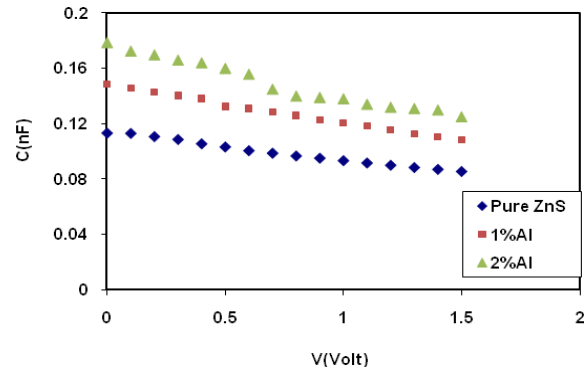


Figure 3: The variation of capacitance as a function of reverse bias voltage for nu doped and doped ZnS/Si HJ

concentration (pure, 1%, 2%)wt). We can see from this table that the W decreases with Al concentration due to increase the carrier concentration by doping, which leading to increase the capacitance, therefore W decreases according to this equation:

$$W = [2 \epsilon_1 \epsilon_2 (V_{bi} - V_a) (N_{A1} + N_{D2})^2 / N_{D2} N_{A1} (\epsilon_1 N_{D2} + \epsilon_2 N_{A1})]^{1/2} \quad (5)$$

This behavior is nearly in agreement with[3,4],

The inverse capacitance squared was plotted against applied reverse bias voltage for n-ZnS/p-Si and n-ZnS:Al/p-Si at different Al concentration (pure, 1%, 2%)wt) as shown in Fig. 4. The plots reveal a straight line relationship which means that the junction was an abrupt type [4]. The intersection ( $1/c^2=0$ ) of the straight line with the voltage axis represents the built-in voltage [3], and table I represents the value of built-in voltage. It is observed from

this table that the value of built in voltage is in general decreases with increasing Al concentration as a result of the increase in capacitance value and the decrease of depletion width. Also from the same figure, one can deduce the carrier concentration from the slope of the straight line from the equation (1). table I represents these values which increase with increasing Al concentration and this value is in agreement with other literatures. Also Salma et al [11] have found that the value of barrier height is 1.9 for Au-ZnS from C-V measurements.

**Table I: The variation of zero bias capacitance, depletion region width, built in voltage and carrier concentrations for nu doped and doped ZnS/Si HJ**

Al wt%	$N_D \times 10^{15} \text{ cm}^{-3}$	$C_0 \times 10^9 \text{ Farad}$	$V_{bi} \text{ Volt}$	$W \text{ } \mu\text{m}$
Pure	1.542	0.113	1.8	0.421
1	1.858	0.148	1.6	0.321
2	2.325	0.176	1.37	0.27

One of the important parameters of HJ measurement is current- voltage characteristics which explains the behavior of the resultant current with the applied forward and reverse bias voltage. Fig. 5 shows I-V characteristics for un doped and doped ZnS/Si HJ at forward and reverse bias voltage for different Al concentration. In general the forward dark current is generated due to the flow of majority carriers and the applied voltage inject majority carriers which leads to decrease the value of built-in potential, and decrease the width of the depletion layer. Then the majority and minority carrier concentration is higher than the intrinsic carrier concentration ( $n_i^2 < n_p$ ) which leading to generate recombination current at the low voltage region (0-0.3V) because that the excitation electrons from V.B to C.B will recombine with the holes which found at the V.B, and this is observed by little increases in recombination current at low voltage region. The tunneling current has been represented at the high voltage region (>0.3V). After that there is a fast exponential increase in the current magnitude with increasing the voltage and this is called diffusion current, which is dominated. Also the reverse bias current which also contain two regions, in the first region (low voltages <0.3V) the current slightly increases with increasing the applied voltage, and the generation current dominates, while at the high voltage region (>0.3V), the current is nearly constant and the diffusion current dominates [3,4].

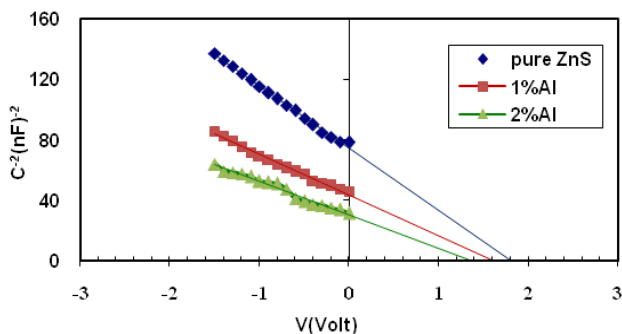


**Figure 4: The variation of  $1/C^2$  as a function of reverse bias voltage for nu doped and doped ZnS/Si HJ**

Also one can observe from this figure that the value of forward current is increases with increasing of Al concentration, which attributed to decrease in the depletion

width (as we see in c-v characteristics), and to improve in crystal structure by increasing Al concentration which attributes to increase in crystallite grain size. Because the increasing of Al concentration will cause rearrangement the interface atoms and reduce the dangling bonds which leads to improve the junction characteristics[5-8]. Fig. 5 shows a clear rectification indicates that the junction is anisotype. The rectification factor (R.F) indicates the ratio between forward and reverse current at certain applied bias voltage, and table II explain the value of rectification factor at (1Volt). The table also shows an increase in rectification with increasing Al concentration, and this is attributed to improve in crystal structure, and the diffusion increases when Al concentration increased [5, 9], Also there is a decrease in depletion width by doping with Al which leading to increase in reverse saturation current, and this value agreement with other literature Huang Jian et al [5,9].

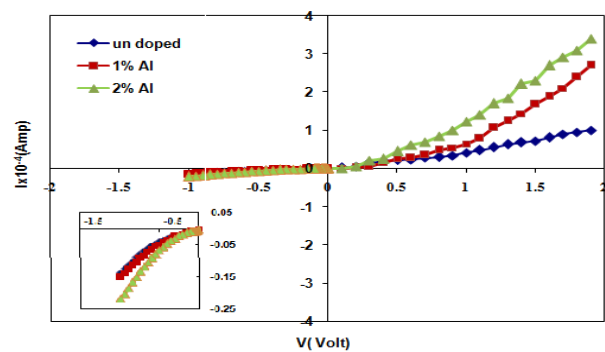


**Figure 5: The I-V characteristics for for un doped and doped ZnS/Si HJ at different Al concentration**

This figure shows that forward current consists of two regions. The first one represents recombination current, while the second region represents tunneling current. The mechanism of the forward current coincides to the tunneling - recombination mechanism. This result is in agreement with results of other researchers [5-10], One can calculate the reverse saturation current from intercept the straight line with the current axis at zero voltage bias, from this figure the reverse saturation current increase with increasing Al concentration. From the first region, the ideality factor ( $\beta$ ) of un doped and doped ZnS/Si HJ can be calculated by the relation [3.4]

$$\beta = (q/k_B T) [V_F / \ln(I_F / I_S)] \quad (6)$$

Where  $V_F$  is the forward bias voltage,  $I_F$  and  $I_S$  are the forward bias and the saturation currents respectively, the ideality factor usually has a value greater than unity, and it describes the deviation of the diode characteristics from those of the ideal diode. table II explains the value of ideality factor for un doped and doped ZnS/Si HJ at different Al concentration. The physical meanings of the ideality factor are greater than (2) is that the tunneling play their role with the recombination emission [3.4]. We can see that the value of ideality factor was varies between 2.58-3.22. These  $\beta$  values are in agreement with Huang Jian et al [5], they found that the value of  $\beta$  varies between (1.9) for un doped ZnS/Si HJ prepared by rf magnetron sputtering method. Wang et al[9], has found that ideality factor is 77 for ZnS/porous Si HJ, and this is due to the roughness of Si. Also Wang et al [10, 11] have found that ideality factor is 81 and 29 for

ZnS/porous Si HJ , and the large value of the ideality factor indicates a high density of trap states. while from the second region, we can find tunneling constant ( $A_t$ ) by the relation:

$$A_t = [d \ln(I_{f2}/I_{s2})]/dv \quad (7)$$

Where  $I_{f2}$  is the forward current for the tunneling region ( $>0.3$ ),  $I_{s2}$  is the saturation current for this region. This value varies between  $4.92-8.05V^{-1}$ , and these values are nearly in agreement with result of [3,4]. The predomination one mechanism on the others was depending on the surface nature of the interface between ZnS and Si. That means, one can observe fast increasing with bias voltage in recombination mechanism, whereas, the variation of tunneling current with voltage was small compared with recombination current, and at high doping the recombination current increases due to increase the carrier at low bias voltage, also the tunneling current increases at high bias voltage due to decrease the width of the depletion layer with increasing bias voltage leads to increase the chance of carrier tunneling.

Table II: The values of rectification factor at (1volt) and ideality factor and tunneling constant.

Al wt%	R.F	$\beta$	$A_t$
Pure	3.018	3.22	4.92
1	4.347	2.93	7.14
2	5.668	2.58	8.05

The photocurrent is considered as the important parameter, which play an effective role in photodetectors and solar cells. The prepared HJ strongly depends on the reverse bias voltage[2]. Fig. 6 show the photocurrent of un doped and doped ZnS/Si HJ at different Al concentration as a function to reverse bias voltage under different incident light power density. The current under reverse bias conditions is affected by illumination [5]. Under UV illumination photons are mainly absorbed in the ZnS layer and ZnS:Al (as seen from the transmittance and absorption spectra [13] and good response to UV illumination under the reverse biased condition can be seen from Fig. 6 due to the photogeneration of additional electron-hole pairs in the depleted ZnS region. The magnitude of photocurrent increases with the increasing applied reverse bias due to enhanced carrier collection. The width of the depletion region increases with the increasing of the applied reverse bias voltage, which leads to separation of the electron-hole pairs and then increases the photocurrent. The photocurrent is a function of the generation and diffusion carriers [13-17]. Also from this figure, we can observe that the photocurrent increases with increasing of the incident light density due to the increasing of the number of incident photon light. Also We can see from this figure that the photocurrent increases with increasing of Al concentration, and this is attributed to good crystalline for the films which will decrease the grain boundary and after that the mobility increases [13], and this is leading to increase the photocurrent. Similar results have also been observed by Mridha and Basak[18] and Jeong et al.[19]

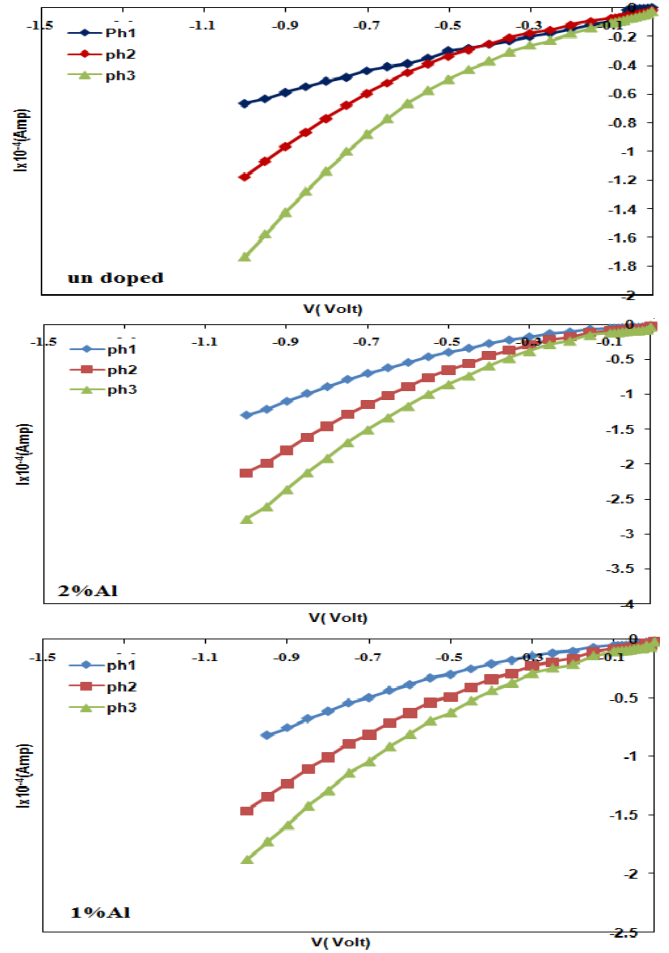


Figure 6: I-V characteristics under illumination for un doped and doped ZnS/Si HJ at different Al concentration

Energy band diagrams for ZnS/Si heterojunctions have been introduced as shown in Fig. 7, by adopting the energy band model of Anderson, neglecting the effects of interface state. From the electrical and optical properties of these heterojunctions [13], it is possible to propose energy band diagrams that give a qualitative account of the experimental results. The total band bending of these heterojunctions can be quantified with the built in potential given by the equation[14,15]:

$$V_{bi} = \phi_1 - \phi_2 = (E_{g1} + \chi_1 - \Delta E_{F1}) - (\chi_2 + \Delta E_{F2}) \quad (8)$$

Where

$$\Delta E_{F1} = E_F - E_V \quad (9)$$

and

$$\Delta E_{F2} = E_C - E_F \quad (10)$$

The values of ( $E_C - E_F$ ) and ( $E_F - E_V$ ) can be calculated from the equations:

$$E_C - E_F = K_B T \ln(N_C / N_D) \quad (11)$$

$$E_F - E_V = K_B T \ln(N_V / N_A) \quad (12)$$

Where

$$N_C = 2(2\pi m_e^* K T / h^2)^{3/2} \quad \text{and} \quad N_V = 2(2\pi m_p^* K T / h^2)^{3/2}$$

The values of the conduction and valence band discontinuities  $\Delta E_C$  and  $\Delta E_V$  have been evaluated by using the following relationships [16,17]:

$$\Delta E_C = \Delta \chi \quad (13)$$

$$\Delta E_V = \Delta E_g - \Delta E_C \quad (14)$$

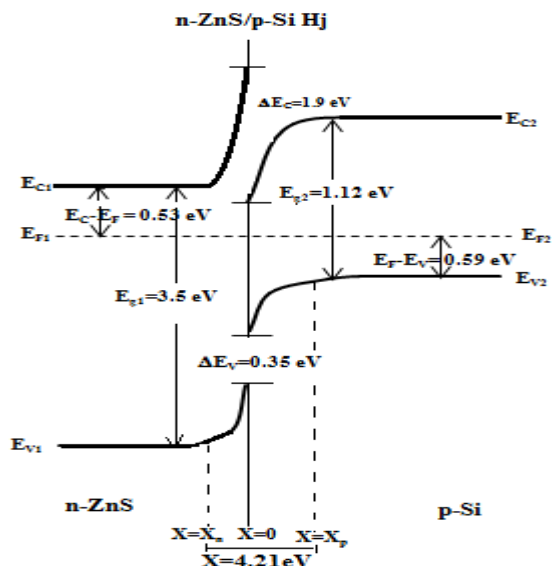


Figure 7: Energy band diagram of n-ZnS/p-Si heterojunction

### CONCLUSIONS

ZnS/Si and ZnS:Al/Si heterojunction thin films have been fabricated successfully by depositing a highly oriented n-type ZnS and ZnS:Al film (1, 2)% Al on a p-type single-crystalline Si substrate using vacuum evaporation technique. The XRD shows that the films exhibit cubic structure oriented in (111) direction. The intensity of the diffraction peak is increased with the addition of Al, which illustrates the enhancement of crystallinity and grain size of ZnS:Al thin films. With the increase of Al concentration, it is observed that the capacitance decreases with increasing the reverse bias, while it increases with increasing Al concentration. The width of the depletion layer decreases with increasing Al concentration. From the inverse capacitance squared plot against applied reverse bias voltage for undoped and doped ZnS/Si HJ at different Al concentrations, the plots reveal a straight line relationship which means that the junction was an abrupt type. It is found that the value of built-in voltage is in general decreases with increasing Al concentration. From C-V measurements, we found that the carrier concentration increases with increasing Al concentration. We deduced from the current-voltage characteristics that the junction has rectification characteristics, and the value of current increases with increasing Al concentration. The mechanism of the forward current coincides with the tunneling-recombination mechanism. The value of ideality factor varies between 2.58-3.22. The physical meanings of the ideality factor being greater than 2 is that the tunneling plays its role with the recombination emission. And the value of the tunneling constant (A) varies between  $4.92-8.05 \text{ V}^{-1}$ . Energy band diagram of ZnS/Si HJ has been constructed.

### ACKNOWLEDGMENT

The authors wish to acknowledge the support rendered by the laboratories of thin films in the physical department, college of science, Baghdad University.

### REFERENCES

[1] K. Jayanthi, S. Chawla, H. Chander, and D. Haranath, Structural, optical and photoluminescence properties of ZnS: Cu nanoparticle thin films as a

function of dopant concentration and quantum confinement effect, *Cryst. Res. Technol.* V.42 (10) (2007) pp. 976 – 982).

[2] T. Ben Nasr, N. Kamoun, M. Kanzari, R. Bennaceur, Effect of pH on the properties of ZnS thin films grown by chemical bath deposition, *Thin Solid Films*, V. 500, (2006) pp.4-8.

[3] B.L.Sharma, R.K.Purohit, "Semiconductors Heterojunctions", Academic Press, Inc, Oxford, New York (1974) pp.1-15.

[4] G.Milnes & D.L.Feucht, "Heterojunctions and Metal Semiconductor Junctions", Academic Press, London (1972).

[5] Huang Jian, Wang Lin-Jun, Tang Ke, Xu Run, Zang Ji-Jun, Lu Xiong-Gang, Xia Yiben, Photoresponse Properties of an n-ZnS/p-Si Heterojunction, *Chin. Phys. Lett.* V. 28, N. 12 (2011) 127301-3.

[6] Liang-Wen Ji, Yu-Jen Hsiao, I-Tseng Tang, Teen-Hang Meen, Chien-Hung Liu, Jenn-Kai Tsai, Tien-Chuan Wu and Yue-Sian Wu, Annealing effect and photovoltaic properties of nano-ZnS/textured p-Si heterojunction, *Nanoscale Research Letters*, V. 8(470) (2013) 1-6

[7] Shiv P. Patel, J.C. Pivin, V.V. Siva Kumar, A. Tripathi, D. Kanjilal, Lokendra Kumar, Grain growth and structural transformation in ZnS nanocrystalline thin films, *Vacuum*, V.85, pp.307-311 (2010).

[8] M. Ashrat, M. Mehmood, A. Qayyum, Influence of source-to-substrate distance on the properties of ZnS films grown by close-space sublimation, *Физика и техника полупроводников*, 2012, том 46, вып. 10

[9] Wang Cai-Feng, Li Qing-Shan, Lv Lei, Zhang Li-Chun, Qi Hong-Xia, Chen Hou, Structural, optical and electrical properties of ZnS/Porous Silicon heterojunction, *Chin. Phys. Lett.*, V.24, N.3(2007)825-827.

[10] Wang Cai-Feng, Li Qing-Shan, Hu Bo, and Li Wei-Bing, The effect of annealing on structural, optical and electrical properties of ZnS/porous silicon composites, *Chinese Physics B*, V. 18, N. 6(2009)2610-14.

[11] Salma M. Shaban, Nada M. Saeed\* and Raad M. S. AL-Haddad, Fabrication and study of zinc sulfide Schottky barrier detectors, *Indian Journal of Science and Technology*, V. 4, N. 4 (April 2011) pp.384-86.

[12] Hai Jun Xia, He Shun Jia, Zhi Tao Yao, Xin Jian Li, Photoluminescence and I-V characteristics of ZnS grown on Silicon nonporous pillar array, *J. Mater. Res.*, V23, N.1(2008)pp.121-126.

[13] Eman M. Nasir., Characterization and Physical Properties of ZnS and ZnS:Al Thin Films", *International journal of Innovative research in science engineering and technology*, To be published, 2014

[14] K. W. Tek, "New Physics (Korean Physical society)", Vol. 14, No. 3, (1974) p. 109 – 13.

[15] A. G. Milnes and D. L. Feucht, "Heterojunctions and Metal-Semiconductor Junctions", Academic Press, New York, (1972).

[16] S. M. Sze and K. Ng. Kwok, "Physics of Semiconductor Devices", 3<sup>rd</sup> ed., John Wiley & Sons, Inc. Hoboken, New Jersey, (2007).

[17] Morgan & K.Board, "An Introduction to Semiconductors Microtechnology", John Wiley & Sons, Inc., New York (1991).

[18] Mridha S and Basak D, *J. Appl. Phys.* V. 101, (2007) 083102

[19] Jeong I S, Kim J H, Park H H and Im S, *Thin Solid Films*, V. 447-448, (2004) pp- 111.



Dr. Eman M. Nasir. Assistant Professor in Physics. She was born in Baghdad, Iraq. She had Ph.D in Thin Films Physics from University of Baghdad, College of Science in 2005. She published more than forty papers in the field of thin films, solar cells, Solid state physics, Semiconductor detectors and characterization of optoelectronic devices.